[Supplementary Information]

Standout electrochemical performance of SnO_2 and Sn/SnO_2 nanoparticles embedded in a KOH-activated carbonized porous aromatic framework (PAF-1) matrix as the anode for lithium-ion batteries

Yan Dong,[a] Saikat Das,[a] Liangkui Zhu,[a] Teng Ben[a]* and Shilun Qiu[a]

[*][a]Department of Chemistry, Jilin University, Changchun, China.

Fax: (+86) 431-85168298

E-mail: tben@jlu.edu.cn

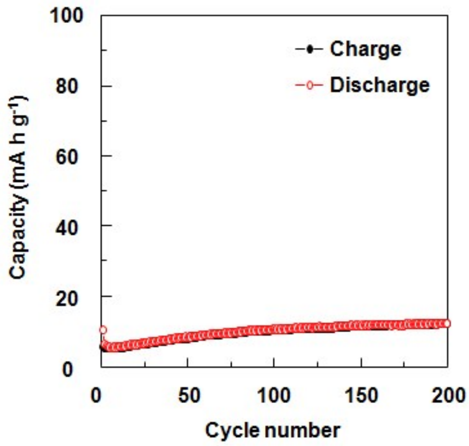

Fig. S1 Cycling performance of PAF-1 showing the charge/discharge capacities at a current density of 200 mA g^{-1} for 200 cycles (the electrodes were prepared by mixing 80 wt% active material and 20 wt% polyvinylidene fluoride (PVDF) binder to form an electrode slurry). The reversible capacity after 200 cycles is 10 mA h g^{-1}. It can be observed that the reversible capacity increases from 2^{nd} to 100^{th} cycles and reach a stable value of about 10 mA h g^{-1} after 100 cycles. This is due to the high microporosity of PAF-1 (reaction between PAF-1 and electrolyte occurs cycle by cycle until the pore is filled with electrolyte).

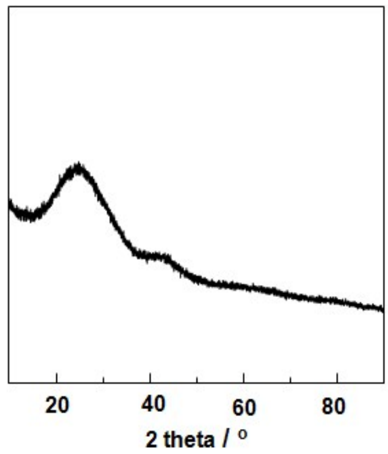

Fig. S2 PXRD pattern of K-PAF-1. The broad peak at 24.0^{o} is ascribed to the (002) diffraction of carbon. The broad peak indicates that K-PAF-1 is essentially amorphous.

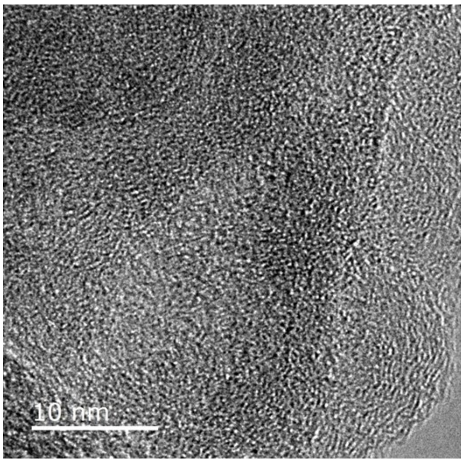

Fig. S3 HRTEM image of K-PAF-1. The high magnification TEM image shows the worm-like structure of K-PAF-1. This is consistent with the result from PXRD analysis.

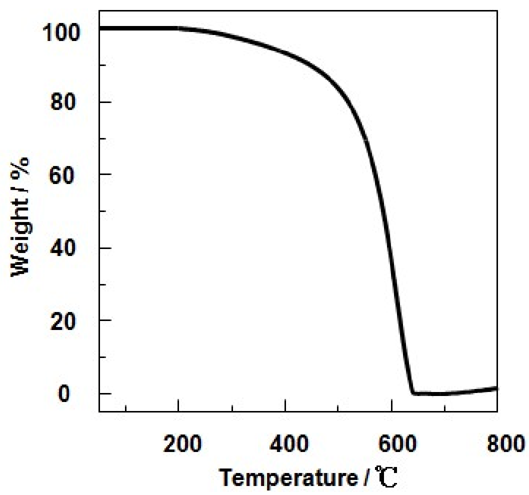

Fig. S4 TGA curve of K-PAF-1. TGA was accomplished under dry air from 50 to 800 ^{o}C at the heating rate of 10 ^{o}C min^{-1}.

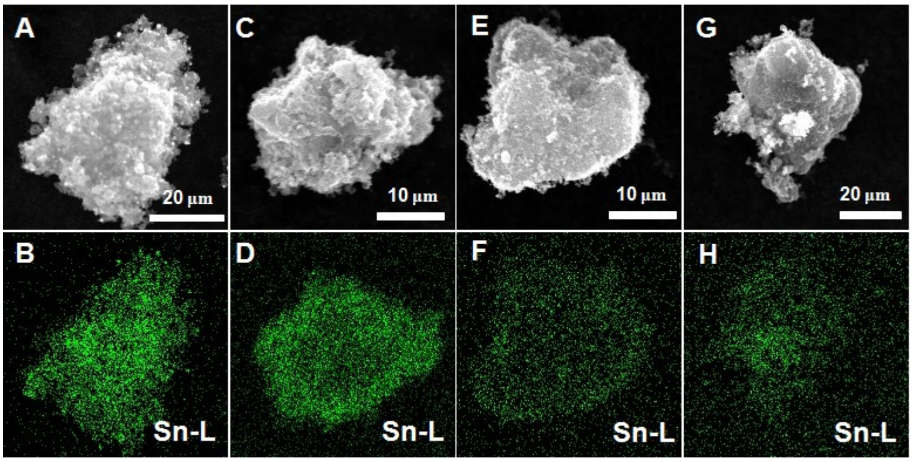

Fig. S5 SEM and corresponding mapping images of SnO_2@K-PAF-1-550 (A, B), SnO_2@K-PAF-1-550-50 (C, D), SnO_2@K-PAF-1-550-25 (E, F) and SnO_2@K-PAF-1-550-10 (G, H). It can be seen that SnO_2 disperses homogeneously in carbon matrix.

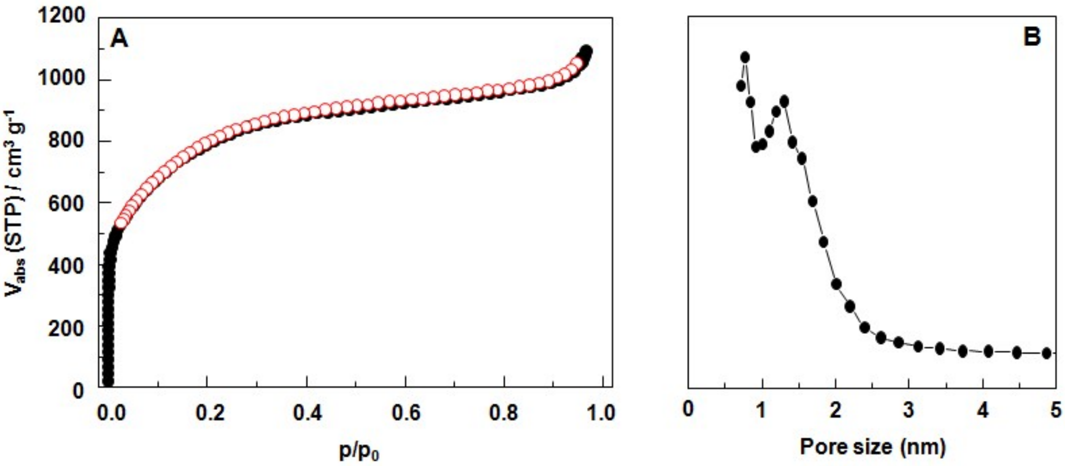

Fig. S6 (A) N_2 sorption (solid symbols, adsorption; open symbols, desorption) and (B) corresponding pore size distribution of K-PAF-1.

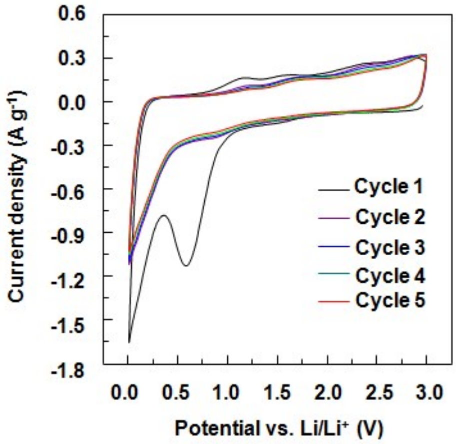

Fig. S7 CV profiles of K-PAF-1 during the first five cycles at a scanning rate of 0.2 mV s^{-1}.

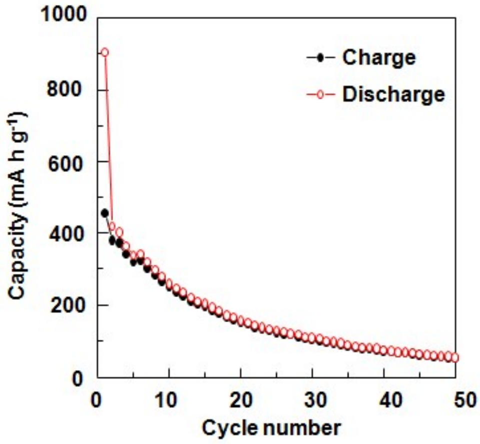

Fig. S8 Cycling performance of commercial SnO_2 showing the charge/discharge capacities at a current density of 200 mA g^{-1} for 50 cycles. The reversible capacity after 50 cycles is 52 mA h g^{-1}.

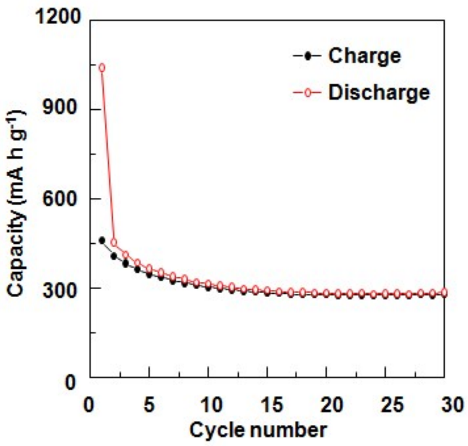

Fig. S9 Cycling performance of K-PAF-1 showing the charge/discharge capacities at a current density of 1000 mA g^{-1} for 30 cycles. The discharge and charge capacities are 1042 and 461 mA h g^{-1} for the first cycle. The reversible capacity after 30 cycles is 281 mA h g^{-1}.

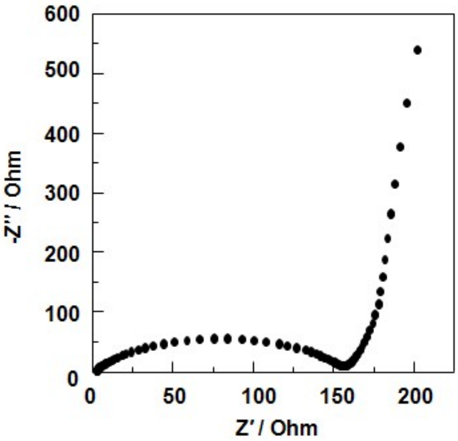

Fig. S10 Electrochemical impedance spectra of K-PAF-1 in the frequency range 100 kHz–0.01 Hz. The charge transfer resistance (R_{ct}) is 156 Ω.

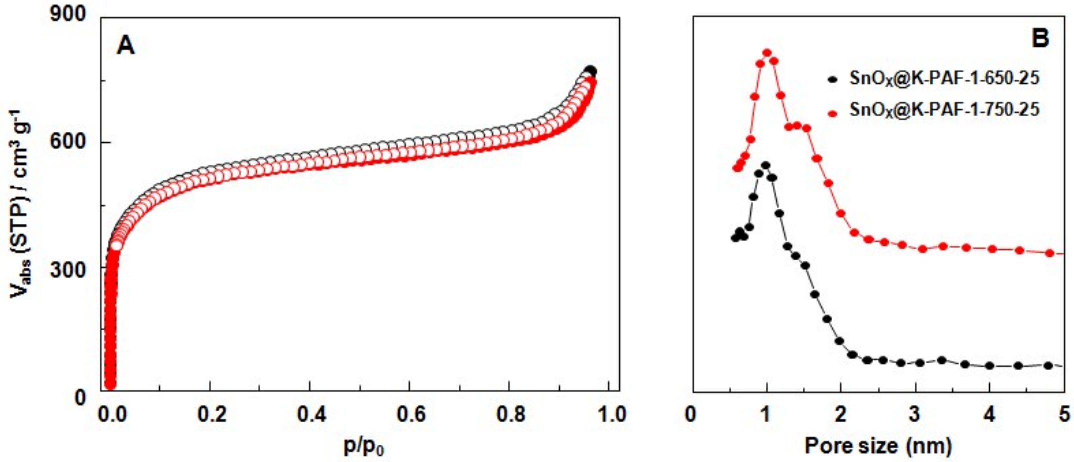

Fig. S11 (A) N_2 sorption (solid symbols, adsorption; open symbols, desorption) and (B) corresponding pore size distribution of SnO_x@K-PAF-1-650-25 and SnO_x@K-PAF-1-750-25.

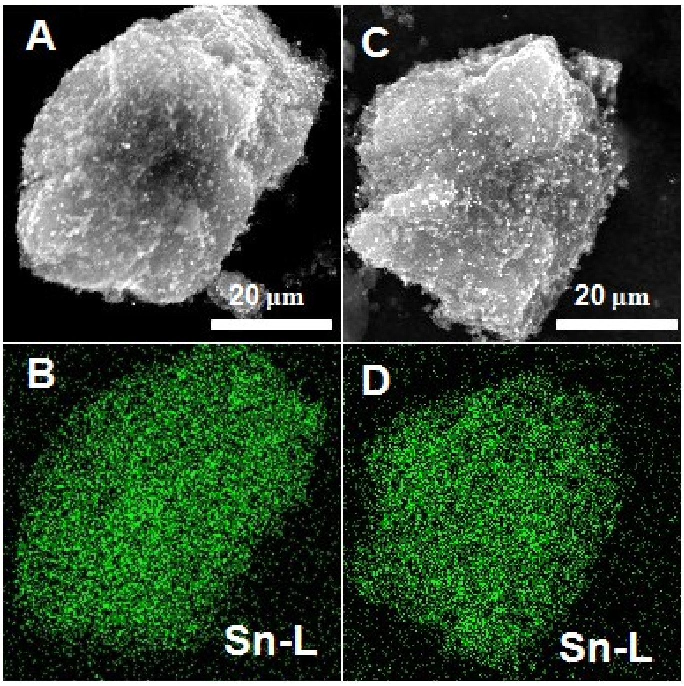

Fig. S12 SEM and corresponding mapping images of SnO_x@K-PAF-1-650-25 (A, B) and SnO_x@K-PAF-1-750-25 (C, D). It can be seen that Sn and SnO_2 disperse homogeneously in carbon matrix.

Table S1 Mass ratio and capacity of all composites.

	SnO_2 (wt%)	Sn (wt%)	K-PAF-1 (wt%)	Theoretical capacity (mA h g^{-1})	Experimental Capacity (mA h g^{-1})
SnO_2@K-PAF-1-550	74.5	-	25.5	701	793
SnO_2@K-PAF-1-550-50	46.5	-	53.5	611	661
SnO_2@K-PAF-1-550-25	21.6	-	78.4	531	784
SnO_x@K-PAF-1-650-25	3.5	21.9	74.6	588	887
SnO_x@K-PAF-1-750-25	0.9	28.5	70.6	615	870
SnO_2@K-PAF-1-550-10	17.0	-	83.0	516	698